Chapter 6
MXene: A Non-oxide Next-Generation Energy Storage Materials for Batteries and Supercapacitors

Mayank Mishra, Sanjay K. Behura, Majid Beidaghi, Kartikey Verma, and Subhash Singh

1 Introduction

The themes of sustainability, carbon neutrality and energy efficiency have spearheaded the increased focus on developing new and advanced renewable sources of energy production and conversion to lay the foundations for next-generation electrochemical and capacitive energy storage devices, an obvious shift from fossil fuel-based systems.

Batteries, a part and parcel of our daily lives, have infused life into both small and big electronics right from microcomputers to electric vehicles and are the predominant energy storage devices. Lithium-ion batteries (LIBs), common household names now because of their easy usability and portability, provide very high energy and power density. There has been a surge in research activities to further enhance performance, efficiency and life cycle of LIBs and other metal-ion batteries by studying and experimenting newer ways of electrode material design, their charge storage mechanisms and manufacturing techniques which could also help bring down the cost of energy production and storage (Mao et al., 2018). Similarly, extensive adaptation of portable electronic and microelectronic systems has hard pressed the need to develop better supercapacitors and microsupercapacitors. Constrained by size, these

M. Mishra · S. Singh (✉)
Department of Production and Industrial Engineering, National Institute of Technology Jamshedpur, Jamshedpur, Jharkhand 831014, India

S. K. Behura
The University of Arkansas at Pine Bluff, Pine Bluff, AR 71601, USA

M. Beidaghi
Department of Mechanical Engineering, Auburn University, Auburn 36849, USA

K. Verma
Department of Chemical Engineering, Indian Institute of Technology, Kanpur 208016, India

S. Singh et al. (eds.), *Advanced Applications of 2D Nanostructures*,
Materials Horizons: From Nature to Nanomaterials,
https://doi.org/10.1007/978-981-16-3322-5_6

are expected to provide higher energy density, higher temperature tolerance, and quick charge and discharge capability with extended life cycles (Fan et al., 2018).

There is one common thread that connects all these seemingly daunting tasks and is at the heart of battery technology. And that is our ability to design and integrate highly compatible materials with exceptional mix of electronic, electrochemical, mechanical and functional properties as electrode material.

In this regard, two-dimensional (2D) materials have revealed tremendous potential by far. Single layer atom thick, they exhibit quite remarkable mechanical, electrical, electronic and chemical properties owing to which they have been able to make deep headways in the fields of semiconductors, electrodes, photovoltaics, water purification, etc. One prominent material among them is graphene, which also holds the distinction of being the first discovered 2D material in 2004, which has come to singlehandedly dominate electronic industry and garnered major research interest.

The year 2011 saw the world being introduced to a new class of 2D materials in the form of MXenes when the first in the family, a non-oxide, layered Ti_3C_2 ceramic was synthesized from its three-dimensional bulk crystalline Ti_3AlC_2 phase by a chemical process known as exfoliation that included selective etching at room temperature and was soon followed by discovery and synthesis of more than a dozen other MXenes structures, an endeavour driven by worldwide skyrocketing demand of high performance energy storage materials for new generation metal-ion batteries and supercapacitors. What impressed researchers about these materials was their interesting mechanical, thermal and electrochemical properties that manifested metal-like electrical and thermal conductivity, ceramic like strength, stiffness and heat resistance together with higher volumetric capacitance and unique structural characteristics which facilitated both effective charge storage and transport (Naguib et al., 2011) (Ghidiu et al., 2014).

2 MXene: A Novel 2D Material

MXenes are novel entrants in the world of two-dimensional materials and are essentially the layered carbides, carbonitrides and very recently nitrides of early transition metals. These are denoted by $M_{n+1}X_n$ ($n = 1, 2, 3$) where 'M' represents an early transition metal (like Sc, Ti, Zr, V, Nb, Cr, Mo) and 'X' represents a carbon or a nitrogen. The 'ene' in MXene draws inspiration from graphene due to its sheet-like structure. They may have more than one 'M' in them which may be arranged as either solid solutions or ordered phases.

Alternatively, in the representation of functionalized MXenes $M_{n+1}X_nT_x$, the additional denotation 'T' refers to free active group (like –H, –F, = O and –OH) surface terminations which are leftovers from the aqueous etchants (HF, H_2O, HCl) used during selective etching of element 'A' from their parent MAX phase. These terminations add hydrophilic nature to the MXenes and strongly influence their electrochemical and dielectric properties. Also, MXene with certain specific terminations

can be achieved via controlled chemical treatment, intercalation and delamination, thermal annealing and exfoliation methods.

The MAX phases are themselves a group of layered structures given as M_nAX_{n+1} ($n = 1$–3) where '*A*' may be one of Al, P, Si, Ga, S, As, Ge, In, Sn, etc. The MAX phase consists of alternate stacked MX layer and '*A*' layer. Selective etching removes the A element, while keeping the MX arrangement unchanged as A element is bonded relatively weaker and is more reactive as compared to very strong M–X bond (Luo, 2018).

Structure wise, MXenes have hexagonal symmetry, a property derived from parent MAX phase lattice structure. MXenes can be prepared in three different forms. One with single *M* element such as Ti_2C and Mo_2C, other existing as a solid solution of one or more *M* elements arranged randomly such as $(Ti, V)_2C_2$ and $(Cr, V)_3C_2$ and finally as double-ordered *M* elements where either a single *M* element layer or two layers of a single *M* element are arranged in between layers of a second M element such as Mo_2TiC_2 and $Mo_2Ti_2C_3$. All of these MXenes can be thus represented as M_2X, M_3X_2 and M_4X3, derived from their corresponding MAX phases M_2AX, M_3AX_2 and M_4AX_3 (Khazaei et al., 2017). Figure 1 shows the structure of these MAX phases and their related MXenes.

The first MXene, titanium carbide Ti_3C_2Tx, the most widely studied MXene, was synthesized, or rather discovered in 2011. The MAX phase Ti_3AlC_2 powders were

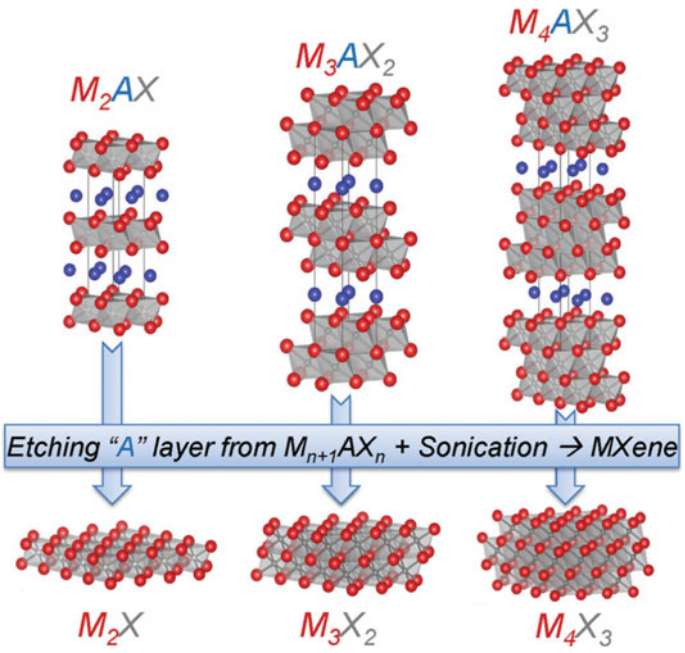

Fig. 1 Structure of different MAX phases and their respective MXenes. 2021 Reproduced with permission from ref. Iqbal et al. (2021). Copyright 2021, Elsevier

mixed with 50 wt. % hydrofluoric acid (HF) solution for 2 h at room temperature.

$$Ti_3AlC_2 + 3HF \rightarrow AlF_3 + 1.5H_2 + Ti_3C_2$$

The following suspension solution was washed with deionized water multiple times, and the powdered precipitate was allowed to settle via centrifuge action.

$$Ti_3C_2 + 2H_2O \rightarrow Ti_3C_2(OH)_2 + H_2$$

$$Ti_3C_2 + 2HF \rightarrow Ti_3C_2F_2 + H_2$$

The above two equations show the formation of MXenes with surface groups, namely OH and F. This process, termed as selective etching process, has been since applied to other precursor MAX phases with the help of other acids as well such as hydrochloric acid (HCl) and lithium fluoride salt (LiF) to synthesize various different MXenes. Upon sonication treatment, MXenes can be delaminated to produce single flake suspensions. Before delamination, MXenes are essentially multilayered structures (Tang et al., 2018). Figure 2 explicitly explains the aforementioned process.

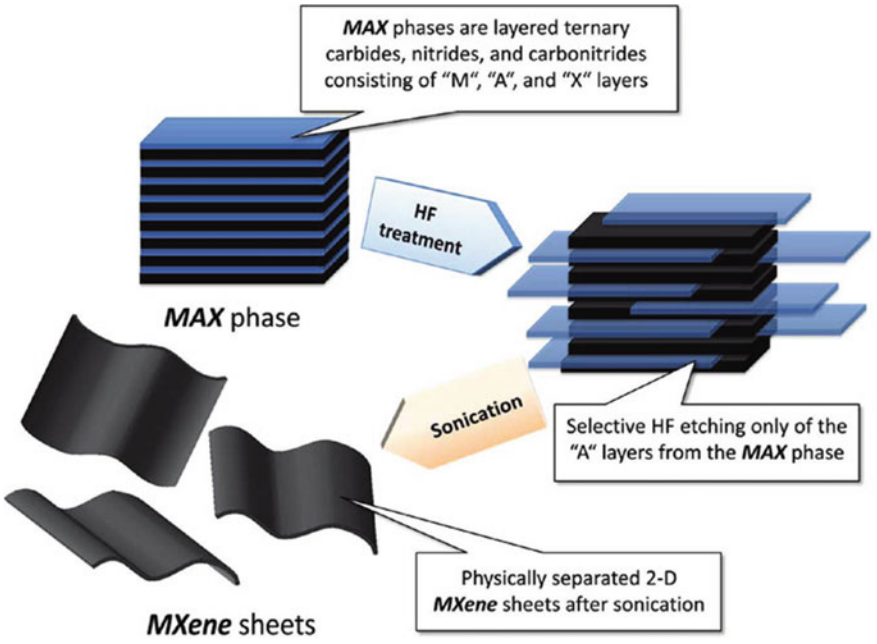

Fig. 2 Schematic for the preparation route of MXenes from the MAX phases. Reproduced with permission from ref. Naguib et al. (2011). Copyright 2012, American Chemical Society

This method was further extended to synthesize other MXenes such as Ti_2C, Ta_4C_3, $(Ti_{0.5}, Nb_{0.5})_2C$, Ti_3CN, $(V_{0.5}, Cr_{0.5})_3C_2$, Ti_2C_3, and Cr_2TiC_2. Alternatively, NH_4HF_2 and mixture of LiF and HCl were also reported to be used as etchants to prepare some MXenes. With time, various endeavours were carried out to produce different MXenes by using different etchants and etching techniques. Needless to say that etching parameters like etching time, etchant concentration, particle size of the MAX phase and temperature during the chemical reactions play crucial parts in the conversion of given MAX phase into MXene. Mo_2C, one of the early transition metal carbides, is the first MXene synthesized from Mo_2Ga_2C phase rather than its MAX phases. Also, Zr_3C_2 MXene was prepared from $Zr_3Al_3C_5$, also not its MAX phase. As of now, over 70 different types of MXenes have been identified and prepared including Ti_3C_2, Ti_2C, V_2C, Cr_3C_2, Fe_2C, Nb_4C_3, Nb_2C, $Mo_{1.33}C$, Mo_2C, Hf_3C_2, V_2C, Cr_2C, Ta_2C, Cr_2N, Ti_4N_3, etc. Many more have been predicted to exist, waiting to be discovered (Zhu et al., 2017).

3 MXene: Properties

MXenes, comparatively the newer entrants into the family of 2D materials, have posed several interesting questions to scientists across disciplines by providing interesting mix of properties. They are both chemically and mechanically stable due to their ceramic nature. Structurally, they are found in both mono-layer and multilayer forms with very large interlayer spacing, even greater than that found in graphite and this thickness of layers can be controlled. This open space between the layers is capable of ion intercalation which means the ions of a range of sizes can be inserted into this space which is very important for the material to be used as cathode in energy conversion applications. Thus, as the layered structure is partially delaminated, not only does it allow ion intercalation but also electric double layer (EDL) formation contributing to charge storage in capacitors. Hydrogen bonding and van der Waals attraction mainly contribute to the interaction between layers of MXenes. The presence of functional groups as terminations provides abundant opportunities for creating desired surface properties and helps control their electrochemical, thermoelectric and dielectric properties. Surface terminations render the otherwise metallic MXenes into semiconductors such as Sc_2CF_2, Sc_2CO_2 and Ti_2CO_2. Moreover, the transition elements (M) in MXenes are very active. Also, a range of transition metals can be used to make the same where each can be tailored for specific applications (Tang et al., 2018; Zhu et al., 2017).

With regards to their mechanical property, it has been estimated by direct functional theory that the in-plane elastic constants of some of these MXenes exceed 500 GPa, which is even more than that of commonly used structural steel which has stiffness value of 400 GPa (Kurtoglu et al., 2012). The electrode material application requires that the MXenes possess very good structural, mechanical, electrochemical, ion movement and electronic transport properties. Their electronic properties are derived from the '*M*' atoms. All the non-functionalized MXenes display metallic

nature, and surface functionalized ones generally display semiconducting nature. Density functional theory (DFT) optimized calculations have shown that Sc-based MXenes such as Sc_2CF_2, $Sc_2C(OH)_2$ and Sc_2CH_2 nanotubes and Mo_2CTx films to have semiconductor-like properties. High conductivity of Ti-based MXenes such as Ti_3C_2Tx was attributed to the Ti vacancy defects. This high conductivity characteristic has put them up for potential application as transparent conductors, electrochemical biosensors, magnetic materials, superconductors, absorbents for heavy metals and flexible electronic devices in addition to their usage in energy storage devices. MXenes have already been experimentally incorporated for potential applications such as rechargeable metal-ion batteries, supercapacitors, field effect transistors, electromagnetic interference shielding, hydrogen storage, sensing, catalysts, composites and biomedical devices among many others. The experimental results have been extremely promising and motivating (Khazaei et al., 2017).

4 MXene for Energy Storage Applications

Aided by modern industrial trends and progressive national policies, as the world transitions from fossil fuel-based energy generation to that derived from renewable sources like wind, sun etc., the need for energy storage devices like electrochemical batteries and supercapacitors is projected to soar higher by the day. They find wide range of applications from portable electronic devices, electric mobility systems to large electric grid systems. Lithium-ion batteries are the most popular form of electrochemical energy storage (EES) systems but they face plethora of challenges as well. These batteries have their own set of safety and cost concerns. They are also marred by very long charging time. It is believed that battery electrode materials have achieved their operational limitations and newer and better devices working on other metal ions like sodium, potassium, magnesium, calcium, etc., are the need of the hour due to their wider and easier availability together with multivalent character. These newer systems also call for improved electrolyte and electrode material development and selection for optimum efficiency (Er et al., 2014).

Of many hurdles facing the growth of LIBs and supercapacitors, two are of extreme significance:

1. It is quite tough to obtain high energy and power density at the same time for these devices.
2. There is an obvious resource crunch with supply chain issues leading to their higher prices (Sun et al., 2018).

Also, the challenge to utilize and store all of the energy produced at larger scales has propelled the scientists to incorporate high performance materials into these devices for optimum efficiency. Working-wise, both rechargeable batteries and supercapacitors have altogether different pros and cons. Batteries produce very high energy densities in expense of poor power densities. Supercapacitors, on other hand, have

superior power densities and fast charge–discharge rate but very low energy densities. Thus, researchers have made immense endeavours to develop electrodes capable of giving a mix of longer life cycle, high energy density and high power density outputs (Xiong et al., 2018). MXenes have been able to help achieve exactly these characteristics. Following are some of the research outputs that establish MXene and MXene-based hybrid structures as the next-generation high-efficient electrode materials for novel batteries and supercapacitors.

4.1 MXenes for Metal-Ion Batteries

Lithium-ion batteries have come to dominate the world of commercial metal-ion-based batteries. They form the backbone of modern-day portable electronic gadgets and are poised for growth in electric vehicles and standalone power storage units. Due to intermittent nature of energy generation of the new renewable energy systems like wind turbines and solar photovoltaics, it becomes increasingly necessary to have a totally reliable storage facility to compensate them in an environmentally sustainable manner devoid of carbon footprints and therein lies the applicability of these rechargeable battery systems.

Of late, they have reached operational ceiling due to lower power density output due to graphite electrodes which is used because of its easy cyclability and low cost. Thus, it was of paramount importance that novel electrode materials be explored for greater electrochemical performance. Also, due to relative scarcity of lithium metal, it is also wise to look for other possible metal based alternatives like battery technologies based on ions of sodium (Na), magnesium (Mg), potassium (K), aluminium (Al) and calcium (Ca). MXenes have come to show their high metal-ion absorption capacity with minimum ion diffusion barrier which arises owing to their high electronic conductivities, greater interlayer spacing and availability of highly active transition metals. $Ti_3C_2T_x$ MXene, the most widely studied MXene in the whole of MXene world, has shown immense promise (Meng et al., 2018a).

Following results discuss the various efforts being put into the development of highly efficient MXene-based rechargeable battery electrodes.

Wang et al. investigated the current collecting capacity of free-standing $Ti_3C_2T_x$ film to replace the conventionally used Al- and Cu-based anode and cathode materials in rechargeable Li-based batteries. For the purpose of the experiment, anode made of multilayer $Ti_3C_2T_x$ and cathode of $LiFePO_4$ was used. The MXene film, in comparison with Cu metal, offered reduction in weight of the battery by about three times. The cyclic voltammograms showed improved Li-ion insertion and extraction in $LiFePO_4$ structure. The high flexibility of the electrode also positioned itself for its applications in flexible electronics (Wang).

Lu et al. studied the effect of reduction in fluorine (−F) surface terminations on the energy storage efficiency of Ti_3C_2 MXene for anode material in lithium-ion batteries. These terminations in large amount significantly brought down Li-ion storage capacity by providing higher diffusion barrier. Thus, hydrogen annealing was

employed to remove excess –F terminations, and the resulting MXene was used as anode in Li-ion battery, it displayed improved volumetric specific capacity of about 123.7 mAh/cm^3 and quite high cycling stability after 100 cycles (Lu et al., 2018).

Du et al. fabricated Ti_2CX_2/graphene hybrid flexible electrode for applications in electrochemically efficient lithium-ion batteries and used first principle method to study its behaviour. It was found that graphene helps avoid restacking of delaminated MXene layers in turn raising its electrical conductivity. The Li-ion mobility was greatly increased which is important for quick ion transport, with high adsorption of Li ions as well. Also, the improved structural stability characterized better structural stiffness (Du et al., 2019).

Zheng et al. employed a microwave irradiation method to uniformly grow carbon nanotubes (CNTs) in situ over Ti_3C_2, Ti_2C and V_2C MXenes to form a hybrid composite structure for potential applications in anode material in Li-ion batteries. The CNT/Ti_3C_2 system showed high reversible capacities of 430 and 175 mAhg^{-1} at current densities of 1 Ag^{-1} and 10 Ag^{-1}, respectively, which is much better than the values for pristine Ti_3C_2. This proved their great potential in energy conversion applications (Zheng et al., 2018).

Kong et al. prepared a nanocomposite mixture of Silicon and Ti_3C_2 MXene with a 1:5 weight ratio via simple ultrasonic mixing to replace traditional Si-based anode in Li-ion batteries. The electrochemical measurements clearly showed the rise in reversible capacity of the composite with 188 mAhg^{-1} at 0.2 Ag^{-1} at the end of 150 cycles as compared to 17 mAhg^{-1} of pure Si. This phenomenon was because of Si-filled interlayer of the Ti_3C_2 MXene (Kong et al., 2018).

Zhao et al. developed an altogether new hybrid composite with MXene/MXene combination of transition metal carbide ($Ti_3C_2T_x$) and transition metal oxides (Co_3O_4 and $NiCo_2O_4$). These were used as anodes in Li ion battery and their electrochemical performance was studied. The $Ti_3C_2Tx/NiCo_2O_4$ electrode fabricated by spray coating showed particularly high rate capacitance of about 1330 mAh/g. Generally speaking, all MXenes composites had improved discharge–charge cycle performance and impressive rate capabilities over standalone parent MXenes (Zhao et al., 2016).

Ali et al. developed two-dimensional nanocomposite heterostructures of iron oxide (Fe_2O_3) and $Ti_3C_2T_x$ MXene for anode material in Li-ion batteries. Composites of varying ratios, i.e. $Ti_3C_2T_x$/25 wt. % Fe_2O_3 and $Ti_3C_2T_x$/50 wt. % Fe_2O_3, were prepared via ball milling, hydrothermal process and wet sonication process; and effect of all these processes was studied. Hydrothermal and wet sonication processes resulted in high oxidation of MXene surface, whereas ball milling produced low surface oxidation and high specific surface area. It was seen that nanocomposite with 50 wt. % Fe_2O_3 prepared via ball milling presented the highest specific energy capacity of about 270 mAhg^{-1} and charge–discharge performance reached 100 mAh/g. Thus, this result showed good promise for their utility in energy storage applications (Ali et al., 2018).

Wang et al. synthesized layered $Li_4Ti_5O_{12}/Ti_3C_2T_x$ MXene composite via in situ method. It provided exemplary Li-ion storage capability and rapid ionic diffusion by reducing the travel path of ions and electrons. Moreover, it manifested high discharge

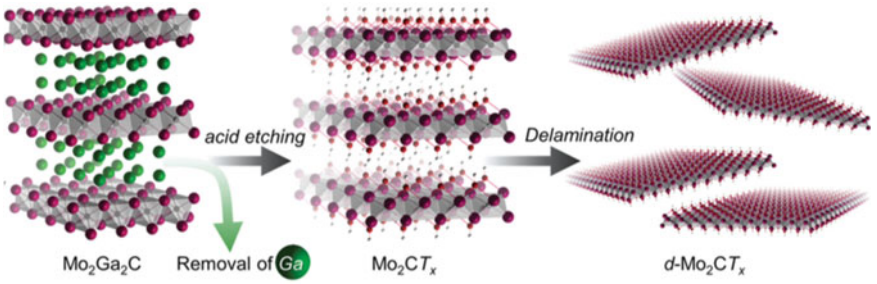

Fig. 3 Schematic of synthesis and delamination process of Mo_2CT_x. Reproduced with permission from ref. Gao, et al. (2020) Copyright 2020, American Chemical Society

capacity with 116 $mAhg^{-1}$ at a rate of 10 Ag^{-1} and high cyclic stability after 500 cycles at 178 $mAhg^{-1}$ (Wang, 2018).

Halim et al. investigated the electrochemical properties of delaminated molybdenum carbide (Mo_2CT_x) MXene prepared from its MAX phase Mo_2Ga_2C by selectively etching out gallium followed by delamination and intercalation with tetrabutylammonium hydroxide (TBAOH) in water, as shown in Fig. 3. The MXene showed semiconductor-like characteristics. It also showed very high capacitance retention upon 10,000 cycles at 10 A/g when tests were carried out on thick Mo_2CT_x film for supercapacitor application. When 8% carbon nanotubes were added into these MXene films to test Li-ion storage capability, over 1000 cycles, it displayed very good cycle performance with reversible capacity of 250 mAh/g (Halim et al., 2016).

Lv et al. have studied the application of delaminated $Ti_3C_2T_x$ MXene in Na-ion batteries. Intercalation and delamination were achieved by ultrasonic treatment in alcohol and dimethyl sulfoxide (DMSO), and a well-developed layered structure was obtained. It was confirmed that delamination led to layer space increase. A relatively higher sodium storage capability was observed in the charge–discharge process while Na-ion insertion into interlayer space concluded the very high rate performance. Cycle performance also confirmed the high stability of the structure of electrodes (Lv et al., 2018).

Meng et al. designed an S-functionalized Ti_3C_2 MXene and investigated the Na-ion storage capacity of Ti_3C_2, $Ti_3C_2O_2$ and $Ti_3C_2S_2$ MXenes to study the changes in storage capabilities with changes in the surface terminations. It was found that $Ti_3C_2S_2$ shows substantially reduced ion diffusion barrier, fast discharge/charge rate and higher Na specific capacity compared to $Ti_3C_2O_2$ mono-layer and thus has an upper hand in terms of electrical conductivity for more efficient electrode material. This was due to large non-positive Na adsorption energies for individual $Ti_3C_2S_2$ layers (Meng, 2018a, 2018b).

Xie et al. developed porous $Ti_3C_2T_x$ MXene electrode via sulphur loading and removal method and analysed its performance for Na-ion storage for practical applications in large-scale Na-ion batteries. It was observed that the ultrathin MXene nanosheets and its open framework due to porous nature facilitated Na-ion storage on its surface. Its volumetric efficiency (216 $mAhcm^{-3}$) was greater than that of

non-porous $Ti_3C_2T_x$ film (64 $mAhcm^{-3}$) at a current density of 100 mAg^{-1}. Thermal annealing helped raise its columbic efficiency to 99% from 96.5% for multilayered $Ti_3C_2T_x$. The rate performance achieved was judged to be the best by far of all previous investigations (Xie et al., 2018).

Tao et al. employed a combination of facile hydrothermal and annealing methods to synthesize $CoNiO_2$ nanoparticles chemically bonded to $Ti_3C_2T_x$ forming a multilayer composite structure. It showed excellent rate capability, electrical conductivity and electrochemical performance which was attributed to the fact that nano size of $CoNiO_2$ helps increase the number of electrochemically active sites and reduces distance for sodium-ion diffusion during discharge–charge cycles (Tao et al., 2018).

Xu et al. synthesized layered composite made of a few nanosheets of MoS_2 on highly conductive $Ti_3C_2T_x$ MXene substrate by one step hydrothermal process for applications in magnesium metal batteries. When used as cathode material, composite showed an increased capacity with 165 mAh/g at 50 mA/g and rate performance was found to be 93 mAh/g at 200 mA/g. It was also evident that Mg-ion charge storage had significantly increased (Xu et al., 2018).

Zhao et al. studied the magnesium-ion storage capacity of porous Ti_3C_2Tx anode films in magnesium-ion storage batteries in Mg-ion-containing electrolyte condition. The cathode performed extremely well in the context of rate performance and cycle consistency. The specific capacitance stood at 210, 140 and 55 $mAhg^{-1}$ at 0.5, 1, and 5 C, making them promising candidates for Mg-ion batteries (Zhao et al., 2019).

Liu et al. demonstrated growth of nickel sulphide (Ni_3S_2) nanofibres on nickel foam by hydrothermal process for the development of binder-less electrode for higher efficiency Na-ion battery. These interconnected nanofibres were able to reduce the diffusion paths of Na ions, thus enhancing the conductivity, specific capacitance, capacity retention and discharge–charge cycle stability. They have proved their suitability to be used as anode material with cathode made of activated carbon due to generation of high energy and power density (Liu et al., 2019).

Mashtalir et al. picked Nb_2CT_x MXene, delaminated it using iso-propylamine and later produced carbon nanotube/MXene composite thin film electrodes and tested it for its lithium storage ability. The CNT/Nb_2CT_x anode exhibited specific capacity of greater than 400 mAh/g at 0.5 C and very high volumetric capacitance of about 325 F/cm^3 (Mashtalir et al., 2015).

Zhu et al. synthesized Ti_3CN nanosheets from the MAX phase Ti_3AlCN for potential application in Na-ion batteries. Its properties were compared with those of Ti_3AlC_2 and Ti_3C_2 nanosheets prepared from the same MAX phase. The electrochemical tests indicated that Na-ion battery based on nanosheets of Ti_3CN had higher specific capacity (507 $mAhg^{-1}$) as compared to that based on Ti_3C_2. Its columbic efficiency reached almost 100% at the end of seven cycles and remained 100% at specific capacity of 139 $mAhg^{-1}$ after 50 cycles while operating at current density of 20 mAg^{-1}. For a test condition of 500 mAg^{-1}, the discharge capacity fared at 98.9 $mAhg^{-1}$ for the electrode made of nanosheets of Ti_3CN, a 1.65 times rise over the value of 59.7 $mAhg^{-1}$ for Ti_3C_2 electrode. This was a clear representation of

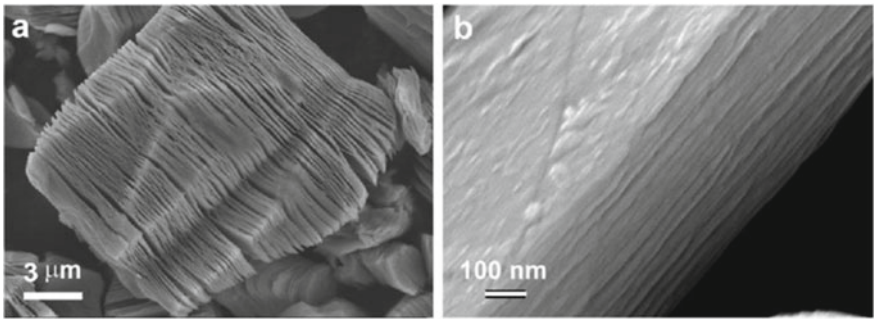

Fig. 4 **a** SEM images of Ti_3CN nanosheets, **b** High magnification SEM images of Ti_3CN nanosheets. Reproduced with permission from ref. Zhu et al. 2018a. Copyright 2018, American Chemical Society

its superior electrochemical efficiency for its use in sodium-ion batteries (Zhu et al., 2018a). Figure 4 shows scanning electron microscopy (SEM) images for Ti_3CN nanosheets at different magnifications.

Meng et al. performed DFT method to quantify the adsorption of Na ions on MXenes of zirconium carbide family, i.e. Zr_2C, Zr_3C_2, Zr_2CO_2, and $Zr_3C_2O_2$. Zr_2C and Zr_3C_2, displayed magnetic nature while Zr_2CO_2 was semiconductor. All of these MXenes displayed metallic behaviour after Na adsorption which is reflective of the rapid electron movement within the electrode in sodium-ion batteries which in turn enhanced the rate capability of the MXene. The combined properties of $Zr_2CO_2/Zr_3C_2O_2$ MXenes like low diffusion barrier, high electrical conductivity, high theoretical values of sodium-ion storage capacity greatly consolidated the confidence that it would make a promising electrode material for Na-ion battery (Meng, 2018).

Du et al. brought about a new method of preparing sulphur cathode in the lithium–sulphur (Li–S) batteries wherein hollow nanospheres of TiO_2 with sulphur additions were embedded into the interlayers of Ti_2C MXene to form a composite cathode. It effectively improved the cathode's cycle performance. With initial discharge specific capacity of 1408.6 $mAhg^{-1}$ at 78.4 wt. % sulphur, after 200 cycles, it was maintained at an impressive 464.0 $mAhg^{-1}$. This was mainly attributed to high conductivity and enhanced volumetric expansion of Ti_2C (Du et al., 2019).

Demiroglu et al. investigated the electrochemical behaviour of hybrid heterostructures of $Sc_2C(OH)_2$/graphene, Ti_2CO_2/graphene and V_2CO_2/graphene and studied the diffusion and adsorption of alkaline sodium, potassium and calcium atoms. The latter two systems showed better metal-ion intercalation and thermal stability. The energy barriers were reduced by half and rate capacities increased as compared to those of only MXene-based structures. These heterostructures systems were thus found suitable for certain low and high voltage applications (Demiroglu et al., 2019).

Yang et al. prepared a flexible composite cathode material made of carbon nanofibres with MoS_2 MXene via electrospinning followed by annealing method for

applications in rechargeable aluminium metal-ion batteries. The composite electrode displayed very good aluminium storage capabilities together with excellent discharge–charge capacity with 293 $mAhg^{-1}$ at current density of 100 mAg^{-1} which was retained up to 126.6 $mAhg^{-1}$ at the end of 200 cycles (Yang et al., 2019). Table 1 summarizes the electrochemical performance of various MXene-based systems for applications in metal-ion batteries.

4.2 MXenes for Supercapacitors

Supercapacitors are capacitors with quite high capacitance lying between those of rechargeable batteries and electrolytic batteries. They have faster charge delivery rate and longer charge–discharge cycle than a typical rechargeable battery. They are famed for their temperature tolerance and the ability to be integrally assembled in tandem with solar cells and batteries.

Broadly speaking, there can be two kinds of supercapacitors, both with different processes of charge storage and transfer. Some supercapacitors do not undergo phase change during operation and instead employ redox reactions, intercalations and electrosorption which are quite fast thus providing greater energy densities. These are called pseudocapacitors and are quite different from electrical double layer capacitors (EDLCs), which primarily operate by forming electrical double layer at the interface of the electrode and electrolyte solution. The more the specific surface area of this interface, the more is its capacitance. EDLCs mainly employ electrodes made from carbon or its derivatives like activated carbon and graphite. Regarding pseudocapacitors, traditional materials like MnO_2, MoO_3, Nb_2O_5, RuO_2, etc., do provide high capacitance, but they lack behind owing to their low electrical conductivity. On this front, MXenes have shown tremendous improvement. Their unique structure and electronic properties make them highly suitable for supercapacitor applications. The interlayer provides large space for unhindered and fast electron movement, and in-depth researches have shown that these materials both on their own and with combination of other heteroatoms have achieved very high volumetric capacitance, structural stability, flexibility and rate performance due to lower ion diffusion barrier and ultrahigh ion storage and delivery (Lukatskaya et al., 2017). Some of these results have been discussed ahead.

Zhang et al. used alkalinizing and annealing to strike out excess surface group terminations from the self-assembled layers of $Ti_3C_2T_x$ MXene film to form the supercapacitor electrode. Upon electrochemical tests, it was evident that the electrode film showed very high volumetric capacitance having value of 1805 Fcm^{-3} at current density of 1 Ag^{-1} and capacitance containment of 98% after 8000 cycles. This was contributed mainly by improvement in number of active sites in the MXene (Zhang et al., 2018).

Li et al. prepared $Ti_3C_2T_x$ MXene film electrode decorated with silver (Ag) nanoparticles aqueous dispersion method. The hybrid material displayed high areal capacitance of 332.2 mF cm^{-2}, good rate performance and cycle stability with 87% after 10,000 cycles (Li et al., 2018).

Table 1 Preparation method, rate performance, specific capacity and retention percentage of various MXene-based electrodes for potential applications in rechargeable batteries

S. no	Author	Materials	Preparation method	Parameters					
				Rate performance		Discharge/charge capability			Retention (%)/cycles
				Discharge capacity ($mAhg^{-1}$)	Current density (Ag^{-1})	Specific capacity ($mAhg^{-1}$)	Current density (Ag^{-1})	Cycles	
1	Lv et al.	$Ti_3C_2T_x$	HF etching, ultrasonication in DMHO	140 70	0.02 1	–	–	–	85.8% / 500 cycles
2	Yang et al.	MoS_2/carbon nanofibres	Electrospinning and annealing	293.2 111.9	0.10 0.25	–	–	–	95% / 200 cycles
3	Liu et al.	Ni_3S_2 nanofibers	Hydrothermal method	584.2 355	0.2 1	–	–	–	91.9% / 100 cycles
4	Lu et al.	Ti_3C_2 films	HF etching, sonication, filtration	–	–	123.7 mAh/cm^3	100 mA/cm^3	100	75% /100 cycles
5	Ali et al.	$Ti_3C_2T_x$/25 wt. % Fe_2O_3	LiF and HCl etching, composite by ball milling	100	2	595 372 348	0.3	1 10 50	–
6	Tao et al.	$CoNiO_2/Ti_3C_2T_x$	HF etching, ultrasonication, hydrothermal reaction	413.4 317.6 248.1 211 188.4	20 50 100 200 300	287 239 222	0.1	2 50 140	–

(continued)

Table 1 (continued)

S. no	Author	Materials	Preparation method	Parameters					
				Rate performance		Discharge/charge capability			Retention (%)/cycles
				Discharge capacity ($mAhg^{-1}$)	Current density (Ag^{-1})	Specific capacity ($mAhg^{-1}$)	Current density (Ag^{-1})	Cycles	
7	Er et al.	Ti_3C_2	HF etching	–	–	447.8 (Li) 351.8 (Na) 191.8 (K) 319.8 (Ca)	–	–	–
8	Xie et al.	Porous $Ti_3C_2T_x$	Sulphur loading and removal method	180 166 124 24	0.1 1 10 100	–	–	–	–
9	Zhao et al.	$Ti_3C_2T_x/NiCo_2O_4$ film	Spray coating	1330 650 350	0.03 1.5 3	–	–	–	–
10	Zhu et al.	Ti_3CN	HF etching	–	–	507 217 133	0.02	1 2 100	–

(continued)

Table 1 (continued)

S. no	Author	Materials	Preparation method	Parameters					
				Rate performance		Discharge/charge capability			Retention (%)/cycles
				Discharge capacity ($mAhg^{-1}$)	Current density (Ag^{-1})	Specific capacity ($mAhg^{-1}$)	Current density (Ag^{-1})	Cycles	
11	Zheng et al.	$CNTs/Ti_3C_2$	HF etching and microwave irradiation	430 175	1 10	–	–	–	–
12	Zhao et al.	Porous $Ti_3C_2T_x$ films	LiF + HCl etching, annealing and magnesium-ion intercalation	210 140 70 55	0.05 0.1 0.3 0.5	–	–	1 2 8 15	–
13	Halim et al.	CNT/Mo_2CT_x	Vacuum–assisted filtration method	250 76	5 10	–	–	–	–
14	Du et al.	$S@TiO_2/Ti_2C$	HF etching of MXene, hydrolysis and calcination for TiO_2 synthesis	879.2 722.0 625.8 576.6 317.7	0.34 0.84 1.67 3.35 8.37	1408.6 741.5 501.1 464	0.34	1 50 100 200	–

(continued)

Table 1 (continued)

S. no	Author	Materials	Preparation method	Parameters					
				Rate performance		Discharge/charge capability			Retention (%)/cycles
				Discharge capacity ($mAhg^{-1}$)	Current density (Ag^{-1})	Specific capacity ($mAhg^{-1}$)	Current density (Ag^{-1})	Cycles	
15	Mashtalir et al.	CNT/Nb_2CT_x	HF etching, amine-assisted delamination	600 270 160	0.1 1 2	–	–	–	–
16	Kong et al.	$Si@Ti_3C_2$	MXene by wet chemical method, composite by mixing, filtration and vacuum drying	–	–	188	0.2	150	–
17	Xu et al.	$MoS_2/Ti_3C_2T_x$	MXene by LiF + HCl etching, composite by hydrothermal process	140 93 53	0.1 0.2 0.5	165 108	0.05	1 50	–

(continued)

Table 1 (continued)

S. no	Author	Materials	Preparation method	Parameters					
				Rate performance		Discharge/charge capability			Retention (%)/cycles
				Discharge capacity ($mAhg^{-1}$)	Current density (Ag^{-1})	Specific capacity ($mAhg^{-1}$)	Current density (Ag^{-1})	Cycles	
18	Wang et al.	$Li_4Ti_5O_{12}/Ti_3C_2T_x$	MXene by HF etching, composite by combination of mixing, stirring, drying and calcination	331 230 175 132 116	0.1 0.5 3 7 10	178	5	500	–

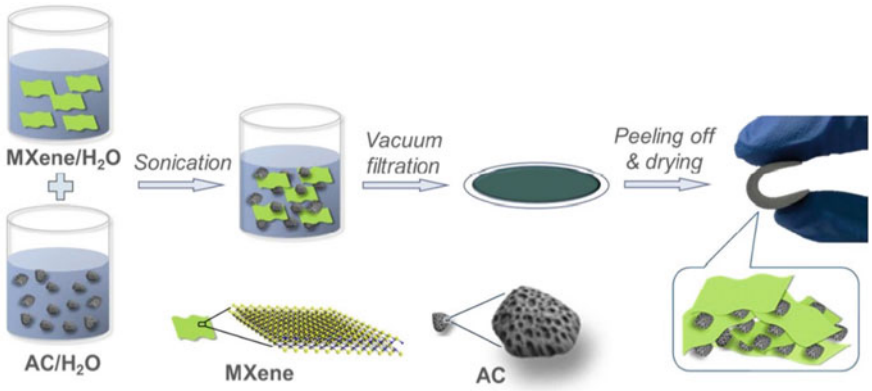

Fig. 5 Schematic representation of fabrication process of MXene-bonded activated carbon films involving sonication of MXene-AC water solution, vacuum filtration, peeling off and drying. Reproduced with permission from ref. Yu et al. Copyright 2018, American Chemical Society

Yu et al. devised a unique fabrication process, as shown in Fig. 5, which involved encapsulating activated carbon in between $Ti_3C_2T_x$ MXene layers via sonication and vacuum filtration followed by peeling off and drying the filtered layers. The MXene layers not only act as flexible backbone but also as binders. The resulting electrode displays very high capacitance of 126 F/g with improved rate performance of 57.9% at 100 A/g. These properties are ideal for its application in flexible supercapacitors (Yu, 2018).

Hu et al. prepared binder-free thick film electrode with pseudocapacitive delaminated $Ti_3C_2T_x$ MXene which were then laser cut to fabricate on-chip microsupercapacitors (MSC) which exhibited areal capacitance of about 71.16 $mFcm^{-2}$ which was a staggering seven times more than the currently used carbon-based on-chip MSCs which measure around 0.1–10 $mFcm^{-2}$ and even greater than previously studied on-chip MSCs pertaining to similar MXene (4.2–61.0 $mFcm^{-2}$), thus making its case formidable for microelectronics applications (Hu et al., 2018).

Chang et al. tried to overcome the stiffness of nano-scale MXene sheets for their application in stretchable and bendable supercapacitors by coming up with alternative electrode design in which certain $Ti_3C_2T_x$ MXene nanocoatings with programmable crumpling and folding were developed. These were then loaded and unloaded at elevated temperatures to embed memory-based deformation characteristics. When these were employed as supercapacitor electrodes, they demonstrated high mechanical stability, high volumetric capacitance and a 27 times increase in areal capacitance when compared to flat MXene electrode. This was in addition to increase in stretchability of 80% in 1D and 225% in 2D (Chang et al., 2018).

Yu et al. assembled lithium-ion capacitor (LIC) with carbon nanotubes (CNTs) filled $Ti_3C_2T_x$ MXene film as anode and activated carbon-made cathode. This composite film displayed excellent reversible capacity (489 $mAhg^{-1}$), cycle stability and performance. The capacity retention of the electrode stood at 83% after 5000 cycles together with high energy density of 67 $Whkg^{-1}$, proving its effectiveness as anode in LICs (Yu et al., 2018a, 2018b).

Zou et al. prepared a composite material for cathodes in supercapacitors by electrostatically assembling α-Fe_2O_3 and $Ti_3C_2T_x$ MXene at room temperature. The resulting composite displayed a range of working potential of 1.2 V with a high specific capacitance of 405.4 and 197.6 Fg^{-1} at current densities of 2 and 20 Ag^{-1}, respectively. Even more significant was its capacitance retention capacity of 97.7% at the end of 2000 cycles which definitely shows immense promise for supercapacitor cathode material (Zou et al., 2018).

Zhu et al. synthesized symmetric $Ti_2CT_x - Ti_2CT_x$ supercapacitor which presented considerable cyclic performance with great power and energy densities. Also, 100% capacitance was retained after 3000 cycles at 20 A/g current density (Zhu et al., 2018b).

Yang et al. reported excellent results from composite electrode made by electrophoretic deposition of carbon nanotubes (CNTs) filled Ti_3C_2 MXene film over graphite paper. The specific capacitance of the electrode was improved by over 1.5 times and 2.6 times with respect to those of pure Ti_3C_2 MXene and CNTs. After 10,000 cycles, the electrode film retained an impressive 100% capacitance. Thus, it helped prove the effectiveness of electrophoretic deposition method of cathode preparation for supercapacitors (Yang et al., 2018).

Yue et al. developed a three-dimensional aerogel structure by ice-template method for microsupercapacitor having $Ti_3C_2T_x$ and reduced graphene oxide as its components. The electrode was covered on its outside with polyurethane which provided excellent self-healing property to the material which was evident from the fact that the device possessed very high capacitance retention of about 81.7% at the end of fifth healing. At the end of 15,000 cycles, 91% charge retention was observed with very high specific capacitance of 34.6 $mFcm^{-2}$ (Yue et al., 2018).

Wen et al. prepared novel $Ti_3C_2T_x$ MXene-based electrodes which were doped with heteroatoms of nitrogen. The electrode showed significantly high capacitances of 192 F/g and 82 F/g in the electrolytic solutions of 1 M H_2SO_4 and 1 M $MgSO_4$, respectively, which were much higher in comparison with undoped MXene which stood at 34 F/g and 52 F/g, respectively (Wen et al., 2017).

Peng et al. investigated the electrochemical performance of an MXene-based solid-state microsupercapacitors where larger and smaller flakes of Mxene $Ti_3C_2T_x$ were made to act as current collector and active material, respectively. The device so fabricated manifested very high areal capacitance peaking at 27.3 $mFcm^{-2}$ and capacitance of 356.8 Fcm^{-2} with retention of capacitance after 10,000 cycles of 100% (Peng et al., 2016).

Jiang et al. fabricated MnO_2 and $Ti_3C_2T_x$ MXene-based hybrid composite electrode which showed tremendous increase in conductivity, specific capacitance, cycle and structural stability. The transfer of electron and diffusion of ions were facilitated by the chemical reaction occurring between the nanoneedles of MnO_2 and layers of $Ti_3C_2T_x$. The energy density peaked very high coupled with amazing 100% retention of capacitance upon 1000 cycles at 0.2 $mAcm^{-2}$ (Jiang et al., 2018).

Shan et al. investigated the electrochemical characteristics of vanadium carbide (V_2C) for supercapacitor application in aqueous condition. The MXene was prepared by HF etching and delaminated using tetramethylammonium hydroxide (TMAOH)

base. Measurements were taken in different electrolyte solutions, namely H_2SO_4, $MgSO_4$ and KOH to garner data on the dependence of its performance on electrolyte medium. The maximum specific capacitance obtained were 487, 184 and 225 F/g in 1 M H_2SO_4, 1 M KOH, and 1 M $MgSO_4$, respectively. That these values were much greater than what had been previously reported gave strong boost to their candidature for supercapacitor electrode application (Shan et al., 2018).

Dall'Agnese et al. sought manufacturing of a Li-ion capacitor based on vanadium carbide (V_2C) Mxene which produced capacitance of about 100 F/g at 0.2 mVs^{-1}. When assembled as a cell with carbon-based cathode and MXene anode, a cell voltage of 3.5 V was obtained (Dall'Agnese et al., 2015). Table 2 summarizes the electrochemical performance of various MXene-based systems for applications in supercapacitors.

5 Conclusion

There is a new buzz in the scientific community about a novel two-dimensional material called Mxene, which after graphene, has attracted many a minds due to its unique mechanical, electrical and primarily electrochemical properties, thus predicting its widespread utility in next-generation highly efficient electrochemical devices for energy storage and delivery which are the need of the hour due to our increasing dependence on small-scale portable electronic devices, medium-scale utility in electric vehicles and large-scale standalone or grid-connected power storage units. Mxene and Mxene-based hybrid structures are being tested for potential electrode materials in both rechargeable battery systems and supercapacitors under variety of aqueous electrolytic solutions on parameters such as power density, energy density, life cycle, charge–discharge cycles, structural stability, volumetric capacitance, areal capacitance, flexibility and deformability, rate performance, ion diffusion barrier, electron mobility, electrical and thermal conductivities. New and improved techniques of etching and post-etching treatments like sonication, annealing, etc., have been developed for optimum intercalation and exfoliation, desired interlayer spacing, removal of excess surface terminations, designed inclusion of dopants and thin and flexible Mxene-based composite films.

As the saying goes, the best way to prepare for the future is to envision and create it. The era of sustainable and carbon neutral energy generation and storage is upon us already, and it requires development of new age materials with unprecedented performance, efficiency and versatility. It demands focussed and coordinated research efforts and planned product development, so that the technology reaches wide spread application at affordable costs to public and at no cost to the nature. And that future is ours to make and is up for grabs!

Table 2 Preparation method, gravimetric/volumetric capacitance, specific capacitance and retention percentage of various MXene-based electrodes for potential applications in supercapacitors

S. no.	Author	Materials	Method	Parameters					
				Gravimetric/volumetric capacitance (Fg^{-1}/Fcm^{-3})	Current density (Ag^{-1})/scan rate (mVs^{-1})	Specific capacitance ($mFcm^{-2}$)	Scan rate (mVs^{-1})	Retention (%)	Cycles
1	Yue et al.	$Ti_3C_2T_x$/graphene aerogel	Freeze drying, reduction and laser cutting	196 120	2 mVs^{-1} 100 mVs^{-1}	34.6	1	91	15,000
2	Dall'Agnese et al.	V_2CT_x	HF etching	–	–	100 F/g	0.2	70	300
3	Halim et al.	Mo_2CT_x	HF etching, TBAOH intercalation	700 F cm^{-3}	2 mVs^{-1}	–	–	100	10,000
4	Lukatskaya et al.	porous $Ti_3C_2T_x$ film	LiF + HCl etching, vacuum filtration	310 210 100	10 mVs^{-1} 10,000 mVs^{-1} 40,000 mVs^{-1}	–	–	–	–
5	Li et al.	Ag/$Ti_3C_2T_x$	Colloidal dispersion, ultrasonication, vacuum filtration	246.2 mF cm^{-2}	2 mVs^{-1}	332.2 209.3	2 100	87	10,000
6	Yu et al.	Activated carbon/$Ti_3C_2T_x$	Minimally intensive layer delamination (MILD) method	126 F g^{-1}	10 mVs^{-1}	138 73	10 4000	92.4	100,000

(continued)

Table 2 (continued)

S. no.	Author	Materials	Method	Parameters					
				Gravimetric/volumetric capacitance (Fg^{-1}/Fcm^{-3})	Current density (Ag^{-1})/scan rate (mVs^{-1})	Specific capacitance ($mFcm^{-2}$)	Scan rate (mVs^{-1})	Retention (%)	Cycles
7	Yu et al.	CNT/$Ti_3C_2T_x$ film	HF etching, delamination by TBAOH, composite by colloidal sonication and filtration	192.6 132.6 54.6	0.1 Ag^{-1} 0.5 Ag^{-1} 2 Ag^{-1}	–	–	81.3	5000
8	Zou et al.	Fe_2O_3/ $Ti_3C_2T_x$	LiF + HCl etching	405.4 197.6	2 Ag^{-1} 20 Ag^{-1}	–	–	97.7	2000
9	Zhang et al.	$Ti_3C_2T_x$	LiF + HCl etching	1805 F cm^{-3}	1 Ag^{-1}	–	–	98	8000
10	Zhu et al.	Ti_2CT_x	HF etching	245 F cm^{-3}	20 Ag^{-1}	517 307	2 100	100	3000
11	Shan et al.	V_2C	HF etching, delamination by TMAOH	487 170	2 mVs^{-1} 100 mVs^{-1}	–	–	83	10,000

(continued)

Table 2 (continued)

S. no.	Author	Materials	Method	Parameters					
				Gravimetric/volumetric capacitance (Fg^{-1}/Fcm^{-3})	Current density (Ag^{-1})/scan rate (mVs^{-1})	Specific capacitance ($mFcm^{-2}$)	Scan rate (mVs^{-1})	Retention (%)	Cycles
12	Yang et al.	CNTs/ Ti_3C_2	LiF + HCl etching, electrophoretic deposition	134	1 Ag^{-1}	–	–	100	10,000
13	Jiang et al.	$MnO_2/Ti_3C_2T_x$	LiF + HCl etching, composite by mild chemical deposition method	130.5	0.2 Ag^{-1}	–	–	90	1000
14	Wen et al.	$N/Ti_3C_2T_x$	HF etching, annealing	128	200 mVs^{-1}	–	–	–	–

Acknowledgements This book chapter was financially supported by Empowerment and Equity Opportunities for Excellence in Science (EEQ/2018/000873), Science & Engineering Research Board (SERB), Department of Science and Technology, Government of India and Ministry of Human Resource and Development (MHRD), Government of India.

References

Ali, A., Hantanasirisakul, K., Abdala, A., Urbankowski, P., Zhao, M.-Q., Anasori, B., Gogotsy, Y., Aissa, B., & Mahmoud, K. A. (2018). Effect of synthesis on performance of MXene/Iron oxide anode material for Lithium-Ion batteries. *Langmuir*.

Chang, T.-H., Zhang, T., Yang, H., Li, K., Tian, Y., Lee, J. Y., & Chen, P.-Y. (2018). Controlled crumpling of two-dimensional titanium carbide (MXene) for highly stretchable, bendable, efficient supercapacitors. *ACS Nano.*

Dall'Agnese, Y., Taberna, P.-L., Gogotsi, Y., & Simon, P. (2015). Two-dimensional vanadium carbide (MXene) as positive electrode for sodium-ion capacitors. *The Journal of Physical Chemistry Letters, 6*(12), 2305–2309.

Demiroglu, I., Peeters, F. M., Gulseren, O., Cakir, D., & Sevik, C. (2019). Alkali metal intercalation in MXene/graphene heterostructures, a new platform for ion battery applications. *The Journal of Physical Chemistry Letters.*

Du, C., Wu, J., Yang, P., Li, S., Xu, J., & Song, K. (2019). Embedding S@TiO_2 nanospheres into MXene layers as high rate cyclability cathodes for lithium-sulphur batteries. *Electrochimica Acta, 295*, 1067–1074.

Er, D., Li, J., Naguib, M., Gogotsi, Y., & Shenoy, V. B. (2014). Ti_3C_2 MXene as a high capacity electrode material for metal (Li, Na, K, Ca) ion batteries. *ACS Applied Materials & Interfaces, 6*(14), 11173–11179.

Fan, Z., Wang, Y., Xie, Z., Xu, X., Yuan, Y., Cheng, Z., & Liu, Y. (2018). A nanoporous MXene film enables flexible supercapacitors with high energy storage. *Nanoscale, 10*(20), 9642–9652.

Gao, L., Li, C., Huang, W., Mei, S., Lin, H., Ou, Q., Zhang, Y., Guo, J., Zhang, F., Xu, S., & Zhang, H. (2020). MXene/polymer membranes: Synthesis, properties, and emerging applications. *Chemistry of Materials 32*(5), 1703–1747.

Ghidiu, M., Lukatskaya, M. R., Zhao, M.-Q., Gogotsi, Y., & Barsoum, M. W. (2014). Conductive two-dimensional titanium carbide 'clay' with high volumetric capacitance. *Nature, 516*, 78–81.

Halim, J., Kota, S., Lukatskaya, M. R., Naguib, M., Zhao, M.-Q., Moon, E. J., Pitock, J., Nanda, J., May, S. J., Gogotsi, Y., & Barsoum, M. W. (2016). Synthesis and characterization of 2D molybdenum carbide (MXene). *Advanced Functional Materials, 26*(18), 3118–3127.

Hu, H., Bai, Z., Niu, B., Wu, M., & Hua, T. (2018). Binder-free bonding of modularized MXene thin films into thick film electrodes for on-chip micro-supercapacitors with enhanced areal performance metrics. *Journal of Materials Chemistry A, 6*(30), 14876–14884.

Iqbal, A., Kwon, J., Kim, M. K., & Koo, C. M. (2021). MXenes for electromagnetic interference shielding: Experimental and theoretical perspectives. *Materials Today Advances, 9*, 100–124.

Jiang, H., Wang, Z., Yang, Q., Hanif, M., Wang, Z., Dong, L., & Dong, M. (2018). A novel $MnO_2/Ti_3C_2T_x$ MXene nanocomposite as high performance electrode materials for flexible supercapacitors. *Electrochimica Acta.*

Khazaei, M., Ranjbar, A., Arai, M., Sasaki, T., & Yunoki, S. (2017). Electronic properties and applications of MXenes: A theoretical review. *Journal of Material Chemistry C, 5*, 2488–2503.

Kong, F., He, X., Liu, Q., Qi, X., Sun, D., Zheng, Y., Wang, R., & Bai, Y. (2018). Enhanced reversible Li-ion storage in Si@Ti_3C_2 MXene nanocomposite. *Electrochemistry Communications, 97*, 16–21.

Kurtoglu, M., Naguib, M., Gogotsi, Y., & Barsoum, M. W. (2012). First principles study of two-dimensional early transition metal carbides. *MRS Communications, 2*(04), 133–137.

Li, L., Zhang, N., Zhang, M., Wu, L., Zhang, X., & Zhang, Z. (2018). Ag-Nanoparticle-decorated 2D titanium carbide (MXene) with superior electrochemical performance for supercapacitors. *ACS Sustainable Chemistry & Engineering, 6*(6), 7442–7450.

Liu, M. C., Li, J., Yang, Q.-Q., Xu, Y., Kong, L.-B., Bai, R.-J., Liu, W., Niu, W., & Chueh, Y.-L. (2019). Hierarchically Interconnected Ni_3S_2 nanofibers as binder-free electrodes for high-performance sodium-ion energy storage devices. *ACS Applied Nano Materials.*

Lu, M., Li, H., Han, W., Chen, J., Shi, W., Wang, J., Meng, X.-M., Qi, J., Li, H., Zhang, W., & Zheng, W. (2018). 2D titanium carbide (MXene) electrodes with lower-F surface for high performance lithium-ion batteries. *Journal of Energy Chemistry.*

Lukatskaya, M. R., Kota, S., Lin, Z., Zhao, M.-Q., Shpigel, N., Levi, M. D., Halim, J., Taberna, P.-L., Barsoum, M. W., Simon, P., & Gogotsi, Y. (2017). Ultra-high-rate pseudocapacitive energy storage in two-dimensional transition metal carbides. *Nature Energy, 2*(8), 17105.

Luo, K., Zha, X.-H., Zhou, Y., Guo, Z., Lin, C.-T., Huang, Q., Zhou, S., Zhang, R., & Du, S. (2018). First-principles study on the electrical and thermal properties of the semiconducting $Sc_3(CN)F_2$ MXene. *RSC Advances, 8*(40), 22452–22459.

Lv, G., Wang, J., Shi, Z., & Fan, L. (2018). Intercalation and delamination of two-dimensional MXene ($Ti_3C_2T_x$) and application in sodium-ion batteries. *Materials Letters, 219*, 45–50.

Mao, J., Zhou, T., Zheng, Y., Gao, H., Liu, H., & Guo, Z. (2018). Two-dimensional nanostructures for sodium-ion battery anodes. *Journal of Materials Chemistry A, 6*(8), 3284–3303.

Mashtalir, O., Lukatskaya, M. R., Zhao, M.-Q., Barsoum, M. W., & Gogotsi, Y. (2015). Amine-assisted delamination of Nb_2C MXene for Li-Ion energy storage devices. *Advanced Materials, 27*(23), 3501–3506.

Meng, Q., Ma, J., Zhang, Y., Li, Z., Hu, A., Kai, J.-J., & Fan, J. (2018a). Theoretical investigation of zirconium carbide MXenes as prospective high capacity anode materials for Na-ion batteries. *Journal of Materials Chemistry A, 6*(28), 13652–13660.

Meng, Q., Ma, J., Zhang, Y., Li, Z., Zhi, C., Hu, A., & Fan, J. (2018b). The S-functionalized Ti_3C_2 Mxene as a high capacity electrode material for Na-ion batteries: a DFT study. *Nanoscale, 10*(7), 3385–3392.

Naguib, M., Kurtoglu, M., Presser, V., Lu, J., Niu, J., Heon, M., Hultman, L., Gogotsi, Y., & Barsoum, M. W. (2011). Two-dimensional nanocrystals produced by exfoliation of Ti_3AlC_2. *Advanced Materials, 23*(37), 4248–4253.

Naguib, M., Mochalin, V. N., Barsoum, M. W., & Gogotsi, Y. (2013). 25th Anniversary article: MXenes: a new family of two-dimensional materials. *Advanced Materials, 26*(7), 992–1005.

Peng, Y.-Y., Akuzum, B., Kurra, N., Zhao, M.-Q., Alhabeb, M., Anasori, B., Kumbur, E. C., Alshareef, H. N., Ger, M.-D., & Gogotsi, Y. (2016). All-MXene (2D titanium carbide) solid-state microsupercapacitors for on-chip energy storage. *Energy & Environmental Science, 9*(9), 2847–2854.

Shan, Q., Mu, X., Alhabeb, M., Shuck, C. E., Pang, D., Zhao, X., Chu, X.-F., Wei, Y., Du, F., Chen, G., Gogotsi, Y., Gao, Y., & Dall'Agnese, Y. (2018). Two-dimensional vanadium carbide (V_2C) MXene as electrode for supercapacitors with aqueous electrolytes. *Electrochemistry Communications.*

Sun, S., Liao, C., Hafez, A. M., Zhu, H., & Wu, S. (2018). Two-dimensional MXenes for energy storage. *Chemical Engineering Journal, 338*, 27–45.

Tang, H., Hu, Q., Zheng, M., Chi, Y., Qin, X., Pang, H., & Xu, Q. (2018). Mxene–2D layered electrode materials for energy storage. *Progress in Natural Science: Materials International, 28*(2), 133–147.

Tao, M., Zhang, Y., Zhan, R., Guo, B., Xu, Q., & Xu, M. (2018). A chemically bonded $CoNiO_2$ nanoparticles/MXene composite as anode for sodium-ion batteries. *Materials Letters, 230*, 173–176.

Wang, C.-H., Kurra, N., Alhabeb, M., Chang, J.-K., Alshareef, H. N., & Gogotsi, Y. (2018a). Titanium carbide (MXene) as a current collector for Lithium-Ion batteries. *ACS Omega, 3*(10), 12489–12494.

Wang, J., Dong, S., Li, H., Chen, Z., Jiang, S., Wu, L., & Zhang, X. (2018b). Facile synthesis of layered $Li_4Ti_5O_{12}$-$Ti_3C_2T_x$ (MXene) composite for high-performance lithium ion battery. *Journal of Electroanalytical Chemistry, 810*, 27–33.

Wen, Y., Rufford, T. E., Chen, X., Li, N., Lyu, M., Dai, L., & Wang, L. (2017). Nitrogen-doped $Ti_3C_2T_x$ MXene electrodes for high-performance supercapacitors. *Nano Energy, 38*, 368–376.

Xie, X., Kretschmer, K., Anasori, B., Sun, B., Wang, G., & Gogotsi, Y. (2018). Porous $Ti_3C_2T_x$ MXene for ultrahigh-rate sodium-ion storage with long cycle life. *ACS Applied Nano Materials, 1*(2), 505–511.

Xiong, D., Li, X., Bai, Z., & Lu, S. (2018). Recent advances in layered $Ti_3C_2T_x$ MXene for electrochemical energy storage. *Small (weinheim an Der Bergstrasse, Germany), 14*(17), 1703419.

Xu, M., Bai, N., Li, H.-X., Hu, C., Qi, J., & Yan, X.-B. (2018). Synthesis of MXene-supported layered MoS_2 with enhanced electrochemical performance for Mg batteries. *Chinese Chemical Letters, 29*(8), 1313–1316.

Yang, L., Zheng, W., Zhang, P., Chen, J., Tian, W. B., Zhang, Y. M., & Sun, Z. M. (2018). MXene/CNTs films prepared by electrophoretic deposition for supercapacitor electrodes. *Journal of Electroanalytical Chemistry.*

Yang, W., Lu, H., Cao, Y., Xu, B., Deng, Y., & Cai, W. (2019). A Flexible Free-standing MoS_2/Carbon Nanofibers Composite Cathode for Rechargeable Aluminum-Ion Batteries. *ACS Sustainable Chemistry & Engineering.*

Yue, Y., Liu, N., Ma, Y., Wang, S., Liu, W., Luo, C., Zhang, H., Cheng, F., Rao, J., Hu, X., Su, J., & Gao, Y. (2018). Highly self-healable 3d microsupercapacitor with MXene–graphene composite aerogel. *ACS Nano, 12*(5), 4224–4232.

Yu, L., Hu, L., Anasori, B., Liu, Y.-T., Zhu, Q., Zhang, P., Gogotsi, Y., & Xu, B. (2018a). MXene-bonded activated carbon as a flexible electrode for high-performance supercapacitors. *ACS Energy Letters, 3*(7), 1597–1603.

Yu, P., Cao, G., Yi, S., Zhang, X., Li, C., Sun, X., Wang, K., & Ma, Y. (2018b). Binder-free 2D titanium carbide (MXene)/carbon nanotube composites for high-performance lithium-ion capacitors. *Nanoscale, 10*(13), 5906–5913.

Zhang, X., Liu, Y., Dong, S., Yang, J., & Liu, X. (2018). Surface modified MXene film as flexible electrode with ultrahigh volumetric capacitance. *Electrochimica Acta, 294*, 233–239.

Zhao, M.-Q., Ren, C. E., Alhabeb, M., Anasori, B., Barsoum, M. W., Gogotsi, Y. (2019). Magnesium-ion storage capability of MXenes. *ACS Applied Energy Materials.*

Zhao, M.-Q., Torelli, M., Ren, C. E., Ghidiu, M., Ling, Z., Anasori, B., Barsoum, M.-W., & Gogotsi, Y. (2016). 2D titanium carbide and transition metal oxides hybrid electrodes for Li-ion storage. *Nano Energy, 30*, 603–613.

Zheng, W., Zhang, P., Chen, J., Tian, W. B., Zhang, Y. M., & Sun, Z. M. (2018). In situ synthesis of CNTs@Ti_3C_2 hybrid structures by microwave irradiation for high-performance anodes in lithium ion batteries. *Journal of Materials Chemistry A, 6*(8), 3543–3551.

Zhu, J., Ha, E., Zhao, G., Zhou, Y., Huang, D., Yue, G., Hu, L., Sun, N., Wang, Y., Lee, L. Y. S., Xu, C., Wong, K., Astruc, D., & Zhao, P. (2017). Recent advance in MXenes: A promising 2D material for catalysis, sensor and chemical adsorption. *Coordination Chemistry Reviews, 352*, 306–327.

Zhu, J., Wang, M., Lyu, M., Jiao, Y., Du, A., Luo, B., Gentle, I., R., & Wang, L. (2018a). Two-dimensional titanium carbonitride MXene for high-performance sodium-ion batteries. *ACS Applied Nano Materials.*

Zhu, K., Jin, Y., Du, F., Gao, S., Gao, Z., Meng, X., Chen, G., Wei, Y., & Gao, Y. (2018b). Synthesis of Ti_2CT_x MXene as electrode materials for symmetric supercapacitor with capable volumetric capacitance. *Journal of Energy Chemistry.*

Zou, R., Quan, H., Pan, M., Zhou, S., Chen, D., & Luo, X. (2018). Self-assembled Mxene ($Ti_3C_2T_x$)/α-Fe_2O_3 nanocomposite as negative electrode material for supercapacitors. *Electrochimica Acta.*